A vector approach for the analysis and synthesis of directional modulation transmitters

A Vector Approach for the Analysis and Synthesis of Directional Modulation Transmitters

Yuan Ding, and Vincent Fusco, *Fellow, IEEE*

***Abstract*— In order to formalize and extend on previous ad-hoc analysis and synthesis methods a theoretical treatment using vector representations of directional modulation (DM) systems is introduced and used to achieve DM transmitter characteristics. An orthogonal vector approach is proposed which allows the artificial orthogonal noise concept derived from information theory to be brought to bear on DM analysis and synthesis. The orthogonal vector method is validated and discussed via bit error rate (BER) simulations.**

***Index Terms*—Artificial orthogonal noise, bit error rate, constellation tracks, directional modulation, orthogonal vector.**

I. Introduction

Wireless technology in many applications is attractive mainly due to its low installation cost, inherent flexibility and scalable nature. However, the lack of a physical boundary surrounding wireless transmission makes confidential information transmitted wirelessly vulnerable to interception. When the presence and location of illegitimate receivers are known to the transmitter, a classical way to prevent interception is to project radiation pattern nulls along the spatial directions where these receivers lie. However, in general, a-priori knowledge about eavesdropper location is impractical since they are non-cooperative nodes. A promising recent technology, directional modulation, (DM), can enhance wireless transmission security.

DM is a transmitter side technology that is capable of projecting digitally encoded information signals into a pre-specified spatial direction while simultaneously distorting the constellation formats of the same signals in all other directions. In [1]-[3] DM structures, which rely on near field diffraction grating interference effects, were described. In these cases the design process is complicated due to the complex interactions in the near field and their spatial dependent transformation into the far field. An effort at DM synthesis was recently made by Daly, [4]-[6]. In [4]-[6] DM architectures consisting of actively driven antenna arrays with reconfigurable phase shifters [4], [7], [8] or radiators [5], [6] under the influence of optimization algorithms, were used for DM synthesis.

A physical layer secure communication architecture, which functions as a DM transmitter, was presented in a US patent [9] in 2001. Here the orthogonality of Walsh waveforms was exploited to generate direction-sensitive pulse position modulation (PPM) signals. An extension of the approach was developed by utilizing the concept of antenna subset modulation (ASM) [10], which, together with the spread-spectrum DM architecture [11], falls into the category of time-modulated arrays [12]-[14]. In [15] quadrature modulated I and Q data streams were separately encoded at the baseband, up-converted to radio frequency (RF) and then separately transmitted. These when combined in the far-field resulted in receive side IQ data de-modulation occurring along a pre-specified spatial direction only.

Despite these works all attempts to date to construct DM transmitters have failed to overcome the various fundamental inherent weaknesses that were manifested in the approaches cited above. Namely, (i) the complex design process [1]-[3], (ii) non-standard modulation formats in the required spatial direction [1]-[8], (iii) inability to spatially re-direct the required secure communication direction [15], and (iv) the need for high-speed RF switches and/or high precision RF phase shifters that can be switched at the signal modulation rate [1]-[14]. All of these factors currently hinder the development and the field use of the DM technique.

In this paper the essence of the DM technique is reappraised.

The structure and the main contributions of this paper are as follows,

1) In Section II, a mathematical model for a one dimensional (1-D) antenna array in free space is presented. It is shown that by releasing a system parameter, namely the gain of the beam-forming network, the DM property can be acquired.
2) In Section III, vector representations of DM systems are introduced. Vector paths and constellation tracks are linked together. With the help of the properties of constellation tracks, the necessary and sufficient condition for achieving DM characteristics is developed. By imposing the vector path constraint during DM system optimization the problem of non-standard modulation formats along the required secured communication direction is resolved.
3) In Section IV, in order to further enhance security level, the concept of orthogonal vectors is proposed. A DM strategy, termed hereafter as dynamic DM, is developed directly from the orthogonal vector concept. Nearly all existing DM systems can be labeled as static DM.
4) In Section V, the orthogonal vector concept is compared with the artificial noise concept studied by the information theory community. The first attempt to link DM systems and artificial noise concepts [16] did not elucidate some important aspects related to DM system design. We now articulate these in this paper. By analyzing the phased DM

Manuscript received May 7, 2013; revised July 11, 2013, and August 26, 2013; accepted September 29, 2013. This work was sponsored by the Queen's University of Belfast High Frequency Research Scholarship.

Y. Ding and V. Fusco are with the Institute of Electronics, Communications and Information Technology (ECIT), Queen's University of Belfast, Belfast BT3 9DT, U.K. (e-mail: yding03@qub.ac.uk; v.fusco@qub.ac.uk).

array in [4] from an artificial noise perspective, we show that previous DM structures are particular RF stage implementation manifestations of artificial noise or orthogonal vector concepts.

5) In Section VI, design procedures for static and dynamic DM transmitter arrays are summarized.
6) In Section VII, a suitable metric for assessing DM systems is discussed.
7) In Section VIII, in order to assess DM system performance obtained post synthesis via the vector approach, BER simulations are conducted under various system settings. It is shown that enhanced directional secrecy performance is achieved at the price of transmitter power efficiency. Further, and for the first time, it is revealed that compared to static DM systems, dynamic DM systems have more consistent BER performance with respect to BER main beam-widths and sidelobe levels irrespective of detailed receiver functional properties. Unlike channel noise which is additive, we show that in dynamic DM systems the injected orthogonal vectors act as multiplicative interference which guarantees the secure communication even when the wireless channel is noise free. Also we show that in dynamic DM systems a secrecy performance tradeoff can be achieved by choosing appropriate 'non-DM' beam steering arrays before orthogonal vector injections.
8) In Section IX, the contributions of this paper are summarized.

Throughout this paper, the following notations will be used: Lowercase with an arrow on top denotes a vector in *x*-*y* plane; Boldface capital letter denotes a complex number, which can also be regarded as a vector in IQ space; Boldface capital letter with an arrow on top denotes a vector, whose elements are complex numbers; $(\bullet)^T$, $(\bullet)^*$ and $(\bullet)^\dagger$ designate transpose, complex conjugate and complex conjugate transpose (Hermitian), respectively; $|\bullet|$ and $\|\bullet\|$ represent modulus of a complex number and norm of a vector; Operator '$\circ$' denotes the Hadamard product of two vectors.

II. 1-D Conventional and DM Array Configurations

The superimposed electric field radiation from a series of N radiating antenna elements at some distant observation point, is given as

$$\boldsymbol{E}(\theta) = \frac{e^{-j\vec{k}\cdot\vec{r}}}{|\vec{r}|} \cdot \begin{bmatrix} \boldsymbol{AP}_1(\theta) \\ \boldsymbol{AP}_2(\theta) \\ \vdots \\ \boldsymbol{AP}_N(\theta) \end{bmatrix}^T \begin{bmatrix} \boldsymbol{A}_1 \cdot e^{j\vec{k}\cdot\vec{x}_1} \\ \boldsymbol{A}_2 \cdot e^{j\vec{k}\cdot\vec{x}_2} \\ \vdots \\ \boldsymbol{A}_N \cdot e^{j\vec{k}\cdot\vec{x}_N} \end{bmatrix} \quad (1)$$

where $\vec{k}$ is the wavenumber vector along the spatial transmission direction, and $\vec{r}$ and $\vec{x}_n$ respectively represent the location vectors of the receiver and the n^{th} array element relative to the array phase center.

For isotropic antenna patterns, i.e., $\boldsymbol{AP}_n(\theta) = 1$, ($n = 1, 2, \ldots, N$), and uniform array element spacing of one half wavelength in a 1-D array, the electric far field component $\boldsymbol{E}$ is determined as,

$$\boldsymbol{E}(\theta) = \sum_{n=1}^{N} \left(\boldsymbol{A}_n \cdot e^{j\pi\left(n-\frac{N+1}{2}\right)\cos\theta} \right) \quad (2)$$

θ is the spatial direction with boresight at 90º. The phase reference is chosen to be the array geometric center.

Generally, in a conventional transmitter prior to radiation by the array elements, information data is modulated digitally at baseband, up-converted, and then identically distributed to each antenna element via a beam-forming network. Since the beam-forming network is linear and usually is made adaptive at the channel fading rate, its complex gain $\boldsymbol{G}_n$ for each n can be regarded as a constant with regards to the modulation rate. Thus modulated far-field electric field $\boldsymbol{E}_m$ is a scaled version (with a complex weights $\boldsymbol{M}$) of modulated data $\boldsymbol{D}_m$ at each direction, (3), where subscript 'm' refers to the m^{th} symbol transmitted. As a consequence the modulation format, namely the constellation patterns in IQ space, is preserved in all spatial directions.

$$\boldsymbol{E}_m(\theta) = \sum_{n=1}^{N} \left(\underbrace{\boldsymbol{D}_m \cdot \boldsymbol{G}_n^*}_{\boldsymbol{A}_{mn}} \cdot e^{j\pi\left(n-\frac{N+1}{2}\right)\cos\theta} \right) = \boldsymbol{D}_m \cdot \underbrace{\sum_{n=1}^{N} \left(\boldsymbol{G}_n^* \cdot e^{j\pi\left(n-\frac{N+1}{2}\right)\cos\theta} \right)}_{\boldsymbol{M}} \quad (3)$$

In order to enhance security level, another degree of freedom can be introduced by varying $\boldsymbol{G}_n$, and hence $\boldsymbol{M}$, at the modulation rate during data transmission, denoted here as $\boldsymbol{G}_{mn}$ and $\boldsymbol{M}_m$ respectively.

In a DM transmitter, $\boldsymbol{G}_{mn}$ is updated at the modulation rate as is $\boldsymbol{D}_m$. Hence $\left(\boldsymbol{D}_m \cdot \boldsymbol{G}_{mn}^*\right)^*$ can be considered as the complex gain, $\boldsymbol{G}_{mn}^{'}$, of a baseband information data controlled beam-forming network, into which an RF carrier f_c, instead of the modulated data stream $\boldsymbol{D}_m$, is injected. $\boldsymbol{D}_m \cdot \boldsymbol{G}_{mn}^*$ can also be regarded as uniquely weighted m^{th} data fed into the n^{th} array element. This weighting is readily implemented at baseband prior to up-conversion if the digital DM architecture proposed in Fig. 1 were to be used.

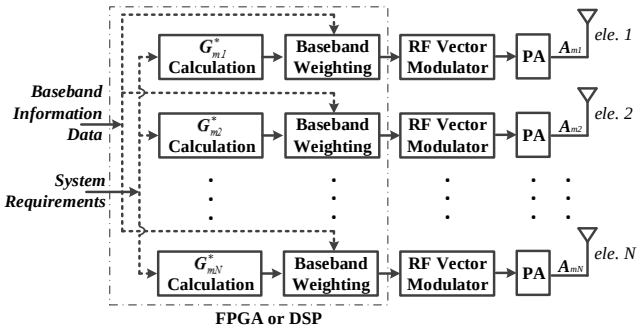

Fig. 1. Illustration of generic digital DM transmitter architecture.

III. Vector Representations for DM Arrays and Constellation Tracks

Since there are different ways to implement a DM system [1]-[14], we require a description technique which is architecture independent and which lends itself to both analysis and synthesis of any class of DM structure. In this section we

analyze the requirements that $\boldsymbol{A}_{mn}$ needs to satisfy for a DM transmitter regardless of the means of how it is generated.

The two key properties of a DM transmitter which we wish to establish are:

- Preservation of the transmitted signal format (standard constellation pattern) along a pre-specified secure communication direction θ_0;
- Distortion of constellation patterns along all other unsecured communication directions.

From the signal processing perspective, $\boldsymbol{E}$ in (2) can be regarded as a constellation point in IQ space, denoted as $\boldsymbol{C}_m$ for the m^{th} symbol transmitted, (4),

$$\boldsymbol{C}_m(\theta) = \sum_{n=1}^{N} \underbrace{\left(\boldsymbol{A}_{mn} \cdot e^{j\pi\left(n-\frac{N+1}{2}\right)\cos\theta} \right)}_{\boldsymbol{B}_{mn}(\theta)} \tag{4}$$

For each symbol transmitted, the vector summation of $\boldsymbol{B}_{mn}$ has to yield the standard constellation point $\boldsymbol{C}_{m\_st}$ in IQ space along, and only along, the direction θ_0. In Fig. 2 two example vector paths selected arbitrarily from the infinite options available are given by way of illustration. Note that these vector paths are different to the phasor diagram [17], in which the excitation strategies are not involved.

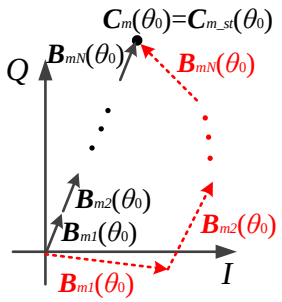

Fig. 2. Examples of two vector paths which reach the same standard constellation point, $\boldsymbol{C}_{m\_st}(\theta_0)$, in IQ space.

From (4), by scanning the observation angle θ, the constellation track in IQ space, $\boldsymbol{C}_m(\theta)$, of the m^{th} symbol can be obtained.

General properties of constellation tracks can be observed from (4),

(a) For an array with odd number elements, constellation tracks are closed loci, in some extreme cases, these loci collapse to line segments, starting point (θ = 0º) always overlaps with end point (θ = 180º). For the case of even number elements, $\boldsymbol{C}_m(0º) = -\boldsymbol{C}_m(180º)$. When the array element spacing is changed, the start and end angle will be changed accordingly;

(b) Changing the desired communication direction θ_0 does not affect the shape of the constellation track pattern, it determines only where the tracks start (θ = 0º) and end (θ = 180º);

(c) Different vector paths inevitably lead to different constellation tracks. This is guaranteed by the orthogonality property of $e^{jn\pi\cos\theta}$ for different n within the spatial range 0º to 180º;

(d) For the q^{th} symbol transmitted, if $\boldsymbol{B}_{qn}(\theta_0)$ are the scaled $\boldsymbol{B}_{mn}(\theta_0)$ with the same scaling factor $\boldsymbol{K}$ for each n, the constellation track $\boldsymbol{C}_q(\theta)$ is also the scaled $\boldsymbol{C}_m(\theta)$ with scaling factor $\boldsymbol{K}$.

Properties (c) and (d) yield that constellation distortion at other directions can be guaranteed if vectors $[\boldsymbol{B}_{q1}(\theta_0)\ \boldsymbol{B}_{q2}(\theta_0)\ \cdots\ \boldsymbol{B}_{qN}(\theta_0)]$ and $[\boldsymbol{B}_{m1}(\theta_0)\ \boldsymbol{B}_{m2}(\theta_0)\ \cdots\ \boldsymbol{B}_{mN}(\theta_0)]$ are linearly independent. Here the q^{th} and the m^{th} symbols in the data stream are different modulated symbols.

Taking QPSK modulation as an example, Fig. 3 (a) illustrates example linearly independent vector paths (N = 5) and the resulting constellation mappings, Fig. 3 (b), for each QPSK symbol when the DM communication direction θ_0 is chosen to be 45º.

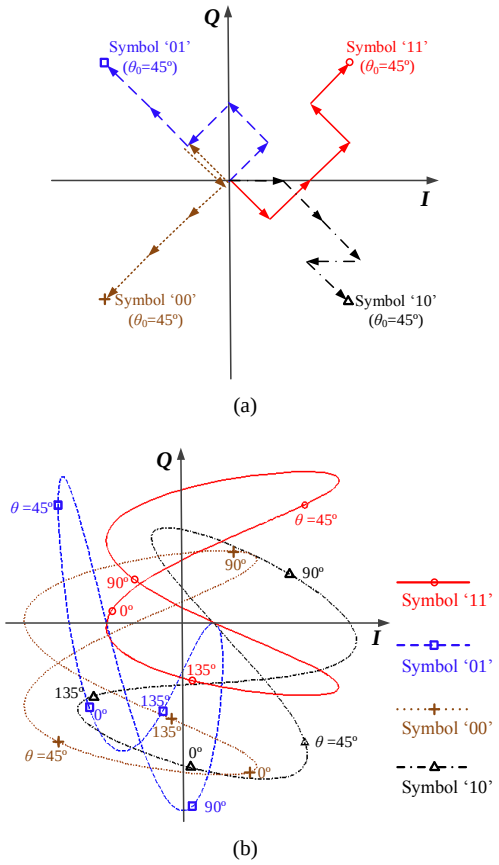

Fig. 3. (a) Example linearly independent vector paths (N = 5) for each QPSK symbol and (b) the corresponding constellation tracks when the DM communication direction θ_0 is chosen to be 45º. 1-D one half wavelength spaced array is assumed.

From the above discussions it can be shown that the DM property is achieved when:

$$\begin{cases} \sum_{n=1}^{N} \boldsymbol{B}_{mn}(\theta_0) = \boldsymbol{C}_{m\_st}(\theta_0) & (5) \\ [\boldsymbol{B}_{q1}(\theta_0)\ \ \boldsymbol{B}_{q2}(\theta_0)\ \ \cdots\ \ \boldsymbol{B}_{qN}(\theta_0)] \\ \quad \neq \boldsymbol{K} \cdot [\boldsymbol{B}_{m1}(\theta_0)\ \ \boldsymbol{B}_{m2}(\theta_0)\ \ \cdots\ \ \boldsymbol{B}_{mN}(\theta_0)] & (6) \end{cases}$$

where $\boldsymbol{K}$ can take any arbitrary complex value and q, m correspond to different modulated symbols.

As a consequence, the requirements for $\boldsymbol{A}_{mn}$ can be obtained via (4).

It needs to be pointed out that if the constraint of vector summation for reaching the standard constellation point at the prescribed direction, (5), is imposed during the DM system optimization (synthesis), one of the major drawbacks of the DM transmitter reported in earlier DM papers, namely not achieving the optimal constellation pattern along the secured direction, is automatically resolved.

IV. Orthogonal Vector Concept

In Section II, we pointed out that a DM transmitter can be constructed by varying, at the modulation rate, $\boldsymbol{G}_n$ and hence $\boldsymbol{M}$ during data transmission in order to release the direct dependence of $\boldsymbol{E}_m$ on $\boldsymbol{D}_m$. Furthermore in Section III, the requirements for the released $\boldsymbol{G}_{mn}$, hence the $\boldsymbol{B}_{mn}$ and $\boldsymbol{A}_{mn}$, were investigated.

If along the DM communication direction each standard constellation point is reached by a fixed vector path, and these vector paths are independent to each other, then DM transmitter functionality will have been synthesized. Since the vector path to each unique constellation point is fixed, this results in a distorted, but static with respect to time, constellation pattern along other spatial directions, hereafter termed 'static DM'. The constellation patterns along all spatial directions can be predicted using the constellation track tool presented in the last section. Nearly all of the DM transmitters reported in the open literature, e.g., [1]-[9] and [15], fall into the static DM category. In static DM systems the constellation patterns are distorted but fixed with respect to time, in all, except the prescribed DM direction, may give eavesdroppers advantage when attempting to recover information.

If the vector paths were randomly re-selected, on a per transmitted symbol basis in order to achieve the same constellation symbol in the desired direction, then the symbol transmitted at the different time slots in the data stream along spatial directions other than the prescribed direction would be scrambled randomly. Equivalently, extra vectors that are orthogonal to the conjugated channel vectors, see Section IV below, could be injected into the system. Here orthogonal vectors are defined as the difference vector between each two vector paths selected to achieve the same standard constellation point in IQ space. This we call the 'dynamic DM' strategy.

A 1-D 5-element array with one half wavelength spacing is taken as an example below to explain the dynamic orthogonal vector approach.

The channel vector for this system operating in free space is

$$\vec{\boldsymbol{H}}(\theta) = \left[\underbrace{e^{j2\pi\cos\theta}}_{\boldsymbol{H}_1} \quad \underbrace{e^{j\pi\cos\theta}}_{\boldsymbol{H}_2} \quad \underbrace{e^{j0}}_{\boldsymbol{H}_3} \quad \underbrace{e^{-j\pi\cos\theta}}_{\boldsymbol{H}_4} \quad \underbrace{e^{-j2\pi\cos\theta}}_{\boldsymbol{H}_5} \right]^T \tag{7}$$

If the excitation signal vectors at the array input, [$\boldsymbol{A}_{m1}$, $\boldsymbol{A}_{m2}$, …, $\boldsymbol{A}_{m5}$], for the same symbol transmitted at the u^{th} and v^{th} time slots are chosen, for example, to be

$$\vec{\boldsymbol{S}}_u = \left[\underbrace{e^{j\left(-\frac{\pi}{4}+2\pi\cos\theta_0\right)}}_{\boldsymbol{S}_{u1}} \quad \underbrace{e^{j\left(\frac{\pi}{4}+\pi\cos\theta_0\right)}}_{\boldsymbol{S}_{u2}} \quad \underbrace{e^{j\left(\frac{\pi}{4}\right)}}_{\boldsymbol{S}_{u3}} \quad \underbrace{e^{j\left(\frac{\pi}{4}-\pi\cos\theta_0\right)}}_{\boldsymbol{S}_{u4}} \quad \underbrace{e^{j\left(\frac{3\pi}{4}-2\pi\cos\theta_0\right)}}_{\boldsymbol{S}_{u5}} \right]^T \tag{8}$$

and

$$\vec{\boldsymbol{S}}_v = \left[\underbrace{e^{j\left(\frac{\pi}{4}+2\pi\cos\theta_0\right)}}_{\boldsymbol{S}_{v1}} \quad \underbrace{e^{j\left(\frac{\pi}{4}+\pi\cos\theta_0\right)}}_{\boldsymbol{S}_{v2}} \quad \underbrace{e^{j\left(-\frac{\pi}{4}\right)}}_{\boldsymbol{S}_{v3}} \quad \underbrace{e^{j\left(\frac{3\pi}{4}-\pi\cos\theta_0\right)}}_{\boldsymbol{S}_{v4}} \quad \underbrace{e^{j\left(\frac{\pi}{4}-2\pi\cos\theta_0\right)}}_{\boldsymbol{S}_{v5}} \right]^T \tag{9}$$

the received vector paths in IQ space along the spatial direction θ_0 are

$$\begin{aligned} \vec{\boldsymbol{B}}_u &= \left[\underbrace{\boldsymbol{H}_1^* \cdot \boldsymbol{S}_{u1}}_{\boldsymbol{B}_{u1}} \quad \underbrace{\boldsymbol{H}_2^* \cdot \boldsymbol{S}_{u2}}_{\boldsymbol{B}_{u2}} \quad \underbrace{\boldsymbol{H}_3^* \cdot \boldsymbol{S}_{u3}}_{\boldsymbol{B}_{u3}} \quad \underbrace{\boldsymbol{H}_4^* \cdot \boldsymbol{S}_{u4}}_{\boldsymbol{B}_{u4}} \quad \underbrace{\boldsymbol{H}_5^* \cdot \boldsymbol{S}_{u5}}_{\boldsymbol{B}_{u5}} \right]^T \\ &= \left[e^{-j\frac{\pi}{4}} \quad e^{j\frac{\pi}{4}} \quad e^{j\frac{\pi}{4}} \quad e^{j\frac{\pi}{4}} \quad e^{j\frac{3\pi}{4}} \right]^T \end{aligned} \tag{10}$$

and

$$\begin{aligned} \vec{\boldsymbol{B}}_v &= \left[\underbrace{\boldsymbol{H}_1^* \cdot \boldsymbol{S}_{v1}}_{\boldsymbol{B}_{v1}} \quad \underbrace{\boldsymbol{H}_2^* \cdot \boldsymbol{S}_{v2}}_{\boldsymbol{B}_{v2}} \quad \underbrace{\boldsymbol{H}_3^* \cdot \boldsymbol{S}_{v3}}_{\boldsymbol{B}_{v3}} \quad \underbrace{\boldsymbol{H}_4^* \cdot \boldsymbol{S}_{v4}}_{\boldsymbol{B}_{v4}} \quad \underbrace{\boldsymbol{H}_5^* \cdot \boldsymbol{S}_{v5}}_{\boldsymbol{B}_{v5}} \right]^T \\ &= \left[e^{j\frac{\pi}{4}} \quad e^{j\frac{\pi}{4}} \quad e^{-j\frac{\pi}{4}} \quad e^{j\frac{3\pi}{4}} \quad e^{j\frac{\pi}{4}} \right]^T \end{aligned} \tag{11}$$

The vector summations in $\boldsymbol{B}_{un}$, and $\boldsymbol{B}_{vn}$ (n = 1, 2, 3, 4, 5) can be calculated as $\vec{\boldsymbol{H}}^{\dagger}(\theta_0)\,\vec{\boldsymbol{S}}_u$ and $\vec{\boldsymbol{H}}^{\dagger}(\theta_0)\,\vec{\boldsymbol{S}}_v$, both reach $3 \cdot e^{j\frac{\pi}{4}}$ in IQ space.

The difference between these two excitation signal vectors is

$$\Delta\vec{\boldsymbol{S}} = \vec{\boldsymbol{S}}_v - \vec{\boldsymbol{S}}_u \tag{12}$$

which is orthogonal to the conjugated channel vector $\vec{\boldsymbol{H}}^*(\theta_0)$ since $\vec{\boldsymbol{H}}^*(\theta_0) \cdot \Delta\vec{\boldsymbol{S}} = 0$. This $\Delta\vec{\boldsymbol{S}}$ is the orthogonal vector defined in this paper.

V. Comparisons Between Orthogonal Vector and Artificial Noise Concepts

The dynamic DM transmitter, when viewed from an information theory aspect, is closely linked to the method of artificial orthogonal vector injection. In the information theory community, artificial orthogonal vector methods, called artificial orthogonal noise, have been developed in order to degrade an eavesdroppers wireless channel even when the physical eavesdropper channel is better than that of the legitimate receiver [18]-[21]. The basic idea, following [20], is as follows;

Design the input signal vector $\vec{\boldsymbol{S}}$ to be

$$\vec{\boldsymbol{S}} = \vec{\boldsymbol{P}}\boldsymbol{X} + \vec{\boldsymbol{W}} \tag{13}$$

Choose $\vec{\boldsymbol{P}}$ to be $\vec{\boldsymbol{H}} \big/ \left\| \vec{\boldsymbol{H}} \right\|$, and update $\vec{\boldsymbol{W}}$ in the null space of $\vec{\boldsymbol{H}}^{\dagger}$ at the information rate. $\vec{\boldsymbol{H}}$ is the channel vector at the desired spatial communication direction. $\boldsymbol{X}$ is a complex

number representing the information to be transmitted.

The received noiseless signal $\boldsymbol{Y}_h$ over the legitimate wireless channel is

$$\boldsymbol{Y}_h = \vec{\boldsymbol{H}}^{\dagger}\vec{\boldsymbol{S}} = \vec{\boldsymbol{H}}^{\dagger}\vec{\boldsymbol{P}}\boldsymbol{X} + \vec{\boldsymbol{H}}^{\dagger}\vec{\boldsymbol{W}} = \left\|\vec{\boldsymbol{H}}\right\|\boldsymbol{X} \tag{14}$$

from which information $\boldsymbol{X}$ can be readily recovered. Although the received $\boldsymbol{Y}_h$ for different $\vec{\boldsymbol{W}}$ is the same, it is achieved by vector summation via different paths, which, as we discussed, endows the system with the ability to scramble constellation patterns along other unsecured channels.

The distorted constellation patterns in other channels can be mathematically verified as

$$\boldsymbol{Y}_z = \vec{\boldsymbol{Z}}^{\dagger}\vec{\boldsymbol{S}} = \vec{\boldsymbol{Z}}^{\dagger}\vec{\boldsymbol{P}}\boldsymbol{X} + \vec{\boldsymbol{Z}}^{\dagger}\vec{\boldsymbol{W}} = \frac{\vec{\boldsymbol{Z}}^{\dagger}\vec{\boldsymbol{H}}}{\left\|\vec{\boldsymbol{H}}\right\|}\boldsymbol{X} + \vec{\boldsymbol{Z}}^{\dagger}\vec{\boldsymbol{W}} \tag{15}$$

$\vec{\boldsymbol{Z}}$ is the eavesdropper's channel vector. Since $\vec{\boldsymbol{W}}$ is not orthogonal to $\vec{\boldsymbol{Z}}^{*}$, the term $\vec{\boldsymbol{Z}}^{\dagger}\vec{\boldsymbol{W}}$ is non-zero, and obfuscates useful information $\boldsymbol{X}$.

Let's now analyze the QPSK DM architecture in [4] from this perspective.

Following (13), we design the input signal vector $\vec{\boldsymbol{S}}_i$ to be

$$\vec{\boldsymbol{S}}_i = A \cdot e^{\frac{(2i-1)\pi}{4}} \cdot \vec{\boldsymbol{P}} + \vec{\boldsymbol{W}}, \quad (i = 1, 2, 3, 4) \tag{16}$$

Since in [4] there is no digital baseband information (signal), A represents the voltage amplitude of the RF carrier f_c at the excitation port of each antenna element. $e^{(2i-1)\pi/4}$ (i = 1, 2, 3, 4 corresponds to each QPSK symbol) represents the information implemented at RF stage, and can be merged into $\vec{\boldsymbol{P}}$ and $\vec{\boldsymbol{W}}$ as,

$$\vec{\boldsymbol{S}}_i = A \cdot \vec{\boldsymbol{P}}_i' + \vec{\boldsymbol{W}}', \quad (i = 1, 2, 3, 4) \tag{17}$$

Choose

$$\vec{\boldsymbol{P}}_i' = e^{\frac{(2i-1)\pi}{4}} \cdot \frac{\vec{\boldsymbol{H}}(\theta_0)}{\left\|\vec{\boldsymbol{H}}(\theta_0)\right\|} = \frac{1}{\sqrt{N}} e^{\frac{(2i-1)\pi}{4}} \cdot \vec{\boldsymbol{H}}(\theta_0) \tag{18}$$

$\vec{\boldsymbol{H}}(\theta_0)$ is similar to (7), but with N items and θ replaced by θ_0. $\vec{\boldsymbol{P}}_i'$ is actually the normalized progressive phase settings with a phase interval $\pi cos\theta_0$. $\vec{\boldsymbol{W}}'$ in (17) can be updated in the null space of $\vec{\boldsymbol{H}}^{\dagger}(\theta_0)$ during the data stream transmission.

With the analysis and synthesis method used in [4] for the same architecture we observe that in [4]:

- a standard QPSK constellation format cannot be consistently formed along a pre-specified communication direction. This is because the constraint in (5) was not imposed during optimization. Alternatively from the artificial orthogonal noise perspective, $\vec{\boldsymbol{P}}_i'$ was not selected to be a constant for each unique QPSK symbol, or equivalently, $\vec{\boldsymbol{W}}'$ was not constrained in the null space of $\vec{\boldsymbol{H}}^{\dagger}(\theta_0)$;
- $\vec{\boldsymbol{W}}'$ is fixed for each unique QPSK symbol. Consequently this is a static DM transmitter;
- if the approach of updating $\vec{\boldsymbol{W}}'$ at the information rate in the null space of $\vec{\boldsymbol{H}}^{\dagger}(\theta_0)$ had been adopted, a dynamic DM transmitter would be forthcoming;

$$\begin{aligned}\vec{\boldsymbol{S}}_i &= A \cdot \vec{\boldsymbol{P}}_i' + \vec{\boldsymbol{W}}' \\ &= \begin{bmatrix} A\boldsymbol{P}_{i1}' & A\boldsymbol{P}_{i2}' & \cdots & A\boldsymbol{P}_{iN}' \end{bmatrix}^T + \begin{bmatrix} \boldsymbol{W}_{i1}' & \boldsymbol{W}_{i2}' & \cdots & \boldsymbol{W}_{iN}' \end{bmatrix}^T \\ &= \begin{bmatrix} A\boldsymbol{P}_{i1}' + \boldsymbol{W}_{i1}' & A\boldsymbol{P}_{i2}' + \boldsymbol{W}_{i2}' & \cdots & A\boldsymbol{P}_{iN}' + \boldsymbol{W}_{iN}' \end{bmatrix}^T \end{aligned} \tag{19}$$

- $\left|A\boldsymbol{P}_{in}' + \boldsymbol{W}_{in}'\right|$ was restricted to be identical for each i and n (i = 1, 2, 3, 4 for each QPSK symbol; n = 1, 2, …, N for each array element), see (19). This indicates that all the array elements have identical transmitted power. This is a consequence of the fact that only one RF chain is used in the analogue DM architecture in [4].
- On the other hand, the artificial orthogonal noise vector method tries to seek the optimum power allocation $\left\|\vec{\boldsymbol{W}}'\right\|^2 / \left\|A\vec{\boldsymbol{P}}'\right\|^2$ in order to achieve the highest secrecy capacity [21]. However the method does not attach any constraint on $\left|A\boldsymbol{P}_{in}' + \boldsymbol{W}_{in}'\right|$. This means that the excitation power at each antenna element can be different, meaning that multiple RF chains are required. This aspect is reflected in the architecture presented in Fig. 1.

When the magnitude of each array element excitation is not uniform, the orthogonal vector approach proposed in this paper and the artificial noise method are differently implemented. Consider now a standard 1-D 5-element Binomial array whose main beam points to boresight (90º). Assume a QPSK symbol '11', $e^{j\pi/4}$, is to be transmitted.

- From the orthogonal vector perspective, the channel vector $\vec{\boldsymbol{H}}_{ov}$, determined solely by the array physical geometry, is defined as

$$\vec{\boldsymbol{H}}_{ov} = \begin{bmatrix} 1 & 1 & 1 & 1 & 1 \end{bmatrix}^T \tag{20}$$

after channel path loss and phase delay are normalized.
In order to receive a signal with unity amplitude, the excitations with Binomial amplitude distribution at the array input should be

$$\begin{aligned}\vec{\boldsymbol{A}} &= \begin{bmatrix} \boldsymbol{A}_{m1} & \boldsymbol{A}_{m2} & \boldsymbol{A}_{m3} & \boldsymbol{A}_{m4} & \boldsymbol{A}_{m5} \end{bmatrix}^T \\ &= \frac{1}{1+4+6+4+1} \cdot \begin{bmatrix} e^{j\frac{\pi}{4}} & 4e^{j\frac{\pi}{4}} & 6e^{j\frac{\pi}{4}} & 4e^{j\frac{\pi}{4}} & e^{j\frac{\pi}{4}} \end{bmatrix}^T \end{aligned} \tag{21}$$

The orthogonal vector is in the null space of $\vec{\boldsymbol{H}}_{ov}^{\dagger}$.

- When examined from the artificial noise perspective recalling (14), we obtain

$$\boldsymbol{Y}_h = \vec{\boldsymbol{H}}_{an}^{\dagger}\vec{\boldsymbol{S}} = \vec{\boldsymbol{H}}_{an}^{\dagger}\vec{\boldsymbol{P}}\boldsymbol{X} + \vec{\boldsymbol{H}}_{an}^{\dagger}\vec{\boldsymbol{W}} = \vec{\boldsymbol{H}}_{an}^{\dagger}\frac{\vec{\boldsymbol{H}}_{an}}{\left\|\vec{\boldsymbol{H}}_{an}\right\|}\boldsymbol{X} \tag{22}$$

$\vec{\boldsymbol{H}}_{an}$ is the channel vector used in artificial noise method. In order to receive a signal with unity amplitude, namely $|\boldsymbol{Y}_h| = 1$, the $\left\|\vec{\boldsymbol{H}}_{an}\right\|$ has to equal 1. Meanwhile the amplitude square

of the elements of $\vec{H}_{an}$ has to follow the Binomial distribution. Hence,

$$\vec{H}_{an} = \frac{1}{\sqrt{16}} \cdot \begin{bmatrix} 1 & \sqrt{4} & \sqrt{6} & \sqrt{4} & 1 \end{bmatrix}^T \tag{23}$$

and

$$\vec{S} = \frac{\vec{H}_{an}}{\left\| \vec{H}_{an} \right\|} X = \frac{1}{\sqrt{16}} \cdot \begin{bmatrix} e^{j\frac{\pi}{4}} & \sqrt{4}e^{j\frac{\pi}{4}} & \sqrt{6}e^{j\frac{\pi}{4}} & \sqrt{4}e^{j\frac{\pi}{4}} & e^{j\frac{\pi}{4}} \end{bmatrix}^T \tag{24}$$

The artificial noise is in the null space of $\vec{H}_{an}^{\dagger}$.

$\vec{H}_{ov}^{\dagger}\vec{A}$ and $\vec{H}_{an}^{\dagger}\vec{S}$ are identical, i.e., $e^{j\pi/4}$, furthermore, the vector path $\vec{H}_{ov}^{*} \circ \vec{A}$ overlaps $\vec{H}_{an}^{*} \circ \vec{S}$. This tells us that while the physical system is the same the channel vectors used for orthogonal vector concept and artificial noise concept can be different. Since $\vec{H}_{ov}$ and $\vec{H}_{an}$ are different, the null space associated with them, in which orthogonal vectors and artificial noise are updated respectively, are different. It should be noted that even if the injected orthogonal vectors and artificial noise are different, the same overall behavior can still be obtained.

To summarize, either the orthogonal vector concept or the artificial noise concept can be utilized to synthesize DM arrays as they have equivalent behavior characteristics. However by separating the excitation strategy from channel vector as used in the orthogonal vector concept we can better reflect the physical arrangement of the system. Furthermore the excitation amplitude of each array element can be obtained in a straightforward manner by summing $\vec{A}$ and the generated orthogonal vector.

VI. Generalized Design Procedures for DM Transmitter Arrays

Based on vector path and orthogonal vector concepts, design procedures for both static and dynamic DM array syntheses are now briefly described,

- Design a 'non-DM' beam steering array. The impact of the choice of beam-forming arrays will be discussed with resulting BER simulations presented in Section VIII.
- For static DM transmitter arrays, the excitation strategy can be obtained by altering the vector path, obtained for the 'non-DM' beam steering array, for each unique modulation symbol under the simultaneous constraint of (5) and (6) as discussed in Section III. Alternatively, it can be achieved by generating linear independent orthogonal vectors for each unique modulation symbol and combining them with the excitations designed in the last step. The array excitations obtained by the orthogonal vector method, as discussed in Section IV, will automatically satisfy (5). The vector paths or orthogonal vectors and system performance can thus be linked, and this mapping can be used for static DM transmitter array optimization against different system performance requirements.
- For dynamic DM transmitter arrays, the array excitation can be obtained by updating orthogonal vectors in the null space of $\vec{H}^{\dagger}(\theta_0)$ at the symbol rate, then combining them with the excitation weights designed in the first step.
- After synthesis the DM system can be implemented using the digital architecture presented in Fig. 1.

In order to further elucidate the design details and several key parameters, the synthesis of a 1-D five element DM array with one half wavelength spacing modulated for QPSK is taken as an example for illustration. Gray coding is adopted in this paper, thus QPSK symbols '11', '01', '00' and '10' should lie in the first to the fourth quadrants in IQ space respectively along the direction pre-assigned for transmission.

In Figs. 4 (a) and (b) the far-field power and phase patterns of a 1-D five element array with uniform excitation magnitude and progressive excitation phase, called hereafter the 'conventional array', for 45º main beam pointing are shown. The identical magnitude and 90º spaced phase for each QPSK symbol indicate a well preserved QPSK constellation pattern, i.e., central-symmetric square, in all spatial directions.

Before synthesizing DM arrays from this conventional beam steering array, two parameters, which are crucial to system performance, need to be discussed. One is the length of each excitation vector. From a practical implementation perspective, the square of the excitation vector should fall into the linear range of each PA located within each RF path, e.g., in Fig. 1. The other is the extra power injected into the 'non-DM' array designed in step one. To describe this extra power we now define the DM power efficiency (PE_{DM}) to be

$$PE_{DM} = \frac{\sum_{i=1}^{I}\left(\sum_{n=1}^{N}\left|\boldsymbol{A}_{in\_nonDM}\right|^2\right)}{\sum_{i=1}^{I}\left(\sum_{n=1}^{N}\left|\boldsymbol{A}_{in\_DM}\right|^2\right)} \times 100\% = \frac{\sum_{i=1}^{I}\left(\sum_{n=1}^{N}\left|\boldsymbol{B}_{in\_nonDM}\right|^2\right)}{\sum_{i=1}^{I}\left(\sum_{n=1}^{N}\left|\boldsymbol{B}_{in\_DM}\right|^2\right)} \times 100\% \tag{25}$$

where I is, for static DM, the number of modulation states, e.g., 4 for QPSK, or, for dynamic DM, the symbol number T in a data stream. $\boldsymbol{A}_{in\_nonDM}$ and $\boldsymbol{A}_{in\_DM}$ are the n^{th} array element excitation for the i^{th} symbol obtained in step one for the non-DM array and in step two or three for the DM array respectively. In noiseless free space, their modulus equal to the normalized modulus of corresponding $\boldsymbol{B}_{in\_nonDM}$ and $\boldsymbol{B}_{in\_DM}$ from the receiver side perspective. Generally the larger the allowable range of the excitation vector lengths and the lower PE_{DM} is, the better the DM system performance that can be achieved. The impact that PE_{DM} has will be illustrated through the BER simulation results presented in Section VIII.

In this paper we adopt the method of generating a fixed set of orthogonal vectors for each unique QPSK symbol for static DM array synthesis, since this facilities the control of PE_{DM}. Denote $\vec{Z}_p$ (p = 1, 2, …, N−1) to be the orthonormal basis in the null space of the normalized $\vec{H}_{ov}^{\dagger}$, then the orthogonal vectors can be designed as $\frac{1}{N-1} \cdot \sum_{p=1}^{N-1}\left(\vec{Z}_p \cdot v_p\right)$. v_p is a random variable. For the i^{th} QPSK symbol

$$PE_{DM\_i} = \frac{1}{1 + \sum_{p=1}^{N-1}\left(\frac{1}{N-1} \cdot v_p\right)^2} \times 100\% \tag{26}$$

and

$$\mathrm{PE}_{\mathrm{DM}} = \frac{1}{I} \cdot \sum_{i=1}^{I} \mathrm{PE}_{\mathrm{DM}\_i} \tag{27}$$

With these relationships we can scale the orthogonal vector in the design process to guarantee a pre-defined $\mathrm{PE}_{\mathrm{DM}}$ to be achieved exactly.

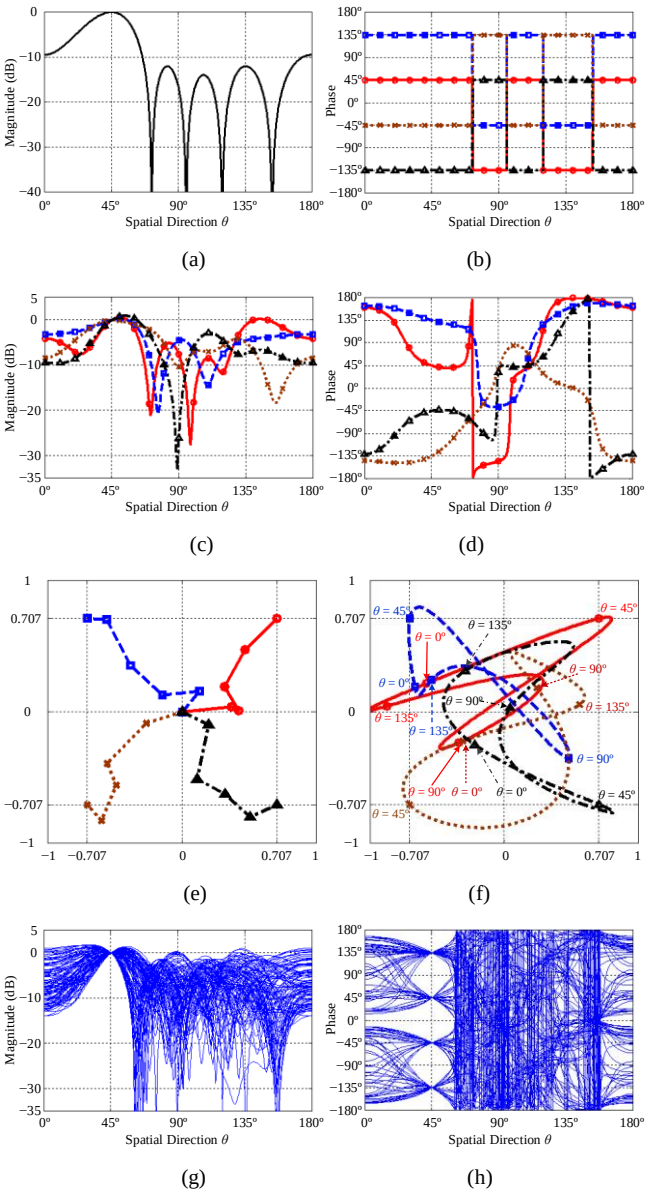

Fig. 4. The far-field (a) power and (b) phase patterns of a conventional array for each QPSK symbol with the main beam steered to 45º; The far-field (c) power and (d) phase patterns of a static DM array for each QPSK symbol with the injected orthogonal vectors listed in Table I; (e) The vector paths and (f) the corresponding constellation tracks for each QPSK symbol in the static DM system; The far-field (g) power and (h) phase patterns of a dynamic DM array for 100 random QPSK symbols. ('—○—': for symbol '11'; '- -□- -': for symbol '01'; '···×···': for symbol '00'; '-·△·-': for symbol '10').

Figs. 4 (c) and (d) depict the far-field power and phase patterns of a static DM transmitter array designed based on the conventional array whose results were given in Figs. 4 (a) and (b). The vector paths of this static DM system for 4 QPSK symbols, which are obtained from the generated orthogonal vectors given in Table I, $\mathrm{PE}_{\mathrm{DM}}$ was set to 50%, and the corresponding constellation tracks are shown in Figs. 4 (e) and (f). It can be seen that the vectors in Table I are orthogonal to the conjugated $\vec{\boldsymbol{H}}(45°)$ in (7).

TABLE I. EXAMPLE ORTHOGONAL VECTORS FOR EACH QPSK SYMBOL IN A STATIC QPSK DM TRANSMITTER ARRAY.

$\vec{\boldsymbol{W}}_{in}$ [a]	Symbol '11' $i = 1$	Symbol '01' $i = 2$	Symbol '00' $i = 3$	Symbol '10' $i = 4$
$\boldsymbol{W}_{i1}$	−0.361−*j*0.424	−0.136−*j*0.595	0.193+*j*0.236	0.055−*j*0.151
$\boldsymbol{W}_{i2}$	0.422+*j*0.085	0.487−*j*0.013	0.501−*j*0.044	0.795−*j*0.035
$\boldsymbol{W}_{i3}$	−0.554+*j*0.099	−0.217+*j*0.189	0.465−*j*0.056	0.146+*j*0.060
$\boldsymbol{W}_{i4}$	0.231−*j*0.205	0.415−*j*0.216	−0.268+*j*0.113	−0.119−*j*0.037
$\boldsymbol{W}_{i5}$	−0.265+*j*0.149	0.289+*j*0.072	−0.586−*j*0.080	−0.547−*j*0.015

$$\vec{\boldsymbol{W}}_{in} = [\boldsymbol{W}_{i1} \quad \boldsymbol{W}_{i2} \quad \boldsymbol{W}_{i3} \quad \boldsymbol{W}_{i4} \quad \boldsymbol{W}_{i5}]^T$$

For dynamic DM transmitter arrays the far-field power and phase patterns for $\mathrm{PE}_{\mathrm{DM}}$ = 50% designed based on the conventional array in Figs. 4 (a) and (b) are presented in Figs. 4 (g) and (h). The number T of transmitted symbols is set to 100. It can be observed from these patterns that the standard QPSK constellation pattern is optimally formed only along the secured communication direction, i.e., 45º in this example, while signal format is scrambled in all other directions.

VII. METRICS FOR ASSESSING A DM SYSTEM

In order to further discuss the DM transmitter synthesis method and evaluate the system performance, a suitable metric for assessing a DM system needs to be investigated.

In [1] and [2] the authors chose 'error rate' as the figure of merit. However the magnitude and phase reference of the detected constellation pattern were not defined. Furthermore channel noise and coding strategy were not considered. These omissions make the 'error rate' of a DM system difficult to systematical assess.

In [4]-[8], [15] a closed form bit-error-rate (BER) equation for QPSK modulation based on 'minimum Euclidean distance decoding' was adopted. However, since BER as a performance metric is defined to a large extent by receiver functionality specifics some further discussion is needed. Firstly we point out that the '$\frac{1}{2}$' before the Q function, repeated here as (28), was erroneously added in previous works [24]; Secondly we comment that with the extra capability of constellation pattern manipulation possessed by a DM transmitter a symbol pair with minimum distance can be a non-Gray-code pair.

$$\mathrm{BER} = \frac{1}{4} \cdot \sum_{i=1}^{4} \left[\frac{1}{2} \cdot Q\left(\sqrt{\frac{(d_i / 2)^2}{N_0 / 2}} \right) \right] \tag{28}$$

Another key aspect preventing the closed form BER equation from being adopted is that distorted noiseless constellation points along unsecured directions can be randomly updated in a dynamic DM system, which makes definitions used for static DM, inapplicable.

Consequently we consider the BER obtained by transmitting

a data stream of random symbols in an AWGN channel an appropriate metric for assessing DM systems. Since BER is also receiver functionality dependent two types of receivers are assumed in this paper. The first is a standard receiver corresponding to the selected digital modulation scheme, e.g., for QPSK a standard receiver decodes received noisy symbols based on which quadrant the constellation points locate into. The second is a more advanced receiver that is able to detect the absolute magnitude and phase of each received symbol. The advanced receiver allows 'minimum Euclidean distance decoding'. In order to obtain magnitude and phase references a training symbol sequence is transmitted via the channel before the data stream. Calculating BER via the data stream approach makes Gray-code inspection for each symbol pair possible. This approach is also applicable for both static and dynamic DM systems.

VIII. Simulation Results and Discussions

In order to assess the DM systems synthesized via the methods presented in Section VI, BER performance under various system settings is obtained. BER simulations are conducted under the following prerequisites:

- QPSK modulation with Gray coding is used;
- A 1-D five isotropic antenna element array with one half wavelength spacing is assumed;
- Unless otherwise specified, a signal to noise ratio (SNR) of 12 dB along the pre-specified secure communication direction, θ_0, is assumed, and the AWGN contribution is identical in all spatial directions. Note that 12 dB is chosen as it permits simulation run lengths of 10^6 symbols to be used and allows BER down to 10^{-5} to be calculated;
- A training sequence with 10^3 random symbols is used. It is assumed that receivers can successfully recover the magnitude and phase references by averaging received signals for each unique symbol state. For standard QPSK receivers, the phase of the averaged received symbol '11' is set as the phase reference, e.g., if the phase of the average received symbol '11' in the training sequence is 60º, each received data symbol in the data stream will be rotated clockwise by (60º − 45º) in IQ space. Then the BER calculation can be carried out by inspecting which quadrant these rotated data symbols lie within. For the advanced QPSK receiver type, four QPSK symbol references are obtained by averaging received training signals. These references are utilized to judge which QPSK symbol the received data signals are then decoded based on the 'minimum Euclidean distance' in IQ space;
- A data stream with 10^6 random QPSK symbols is used for BER simulations.

In Fig. 5 BER spatial distributions detected by standard QPSK receivers in static DM systems for 45º secure communication are presented. For consistency the orthogonal vectors in Table I are used but with different scaling factors in order to satisfy different PE_{DM} requirements. As expected a narrower low BER transmission beam is obtained at the price of lower power efficiency. The BER performance along unsecured directions is largely at approximately the same level as that of a conventional non-DM system, which itself can be considered as a special case of the DM system with a PE_{DM} of 100%. It is noted that the BER along the secured direction, 45º, is well predicted as $BER = Q\left(\sqrt{SNR}\right)$ [22], 3.43×10^{-5} in this example.

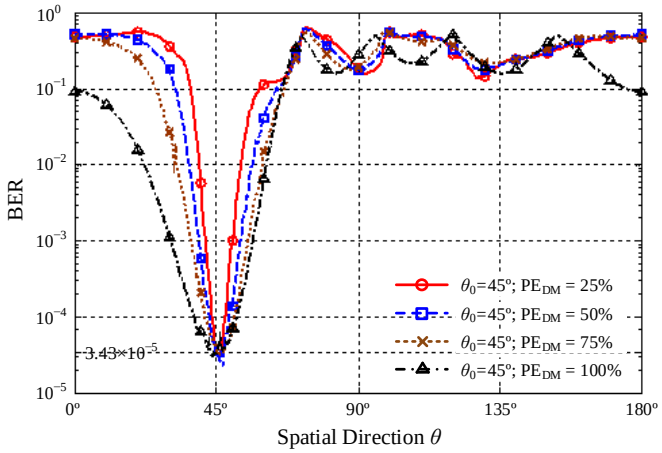

Fig. 5. BER spatial distributions detected by standard QPSK receivers for static DM systems, designed based on the conventional array and the orthogonal vectors in Table I, with different PE_{DM}s for 45º secure communication.

The BER performance of the same static DM systems with the standard QPSK receiver replaced by the advanced version is depicted in Fig. 6. Generally it can be seen that, even though a performance advantage is maintained, the more sophisticated the receiver the less the DM performance advantage becomes with regards to BER main beam-widths and sidelobe levels. In Fig. 6 another interesting trend can be observed, i.e., low PE_{DM} leads only to a slightly narrower BER beam accompanied with a shift in the BER main beam pointing direction and lower averaged BER along other undesired directions. This occurs mainly because larger received power can compensate the adverse impact of distorted constellation patterns on BER under the premise of advanced receiver recovery.

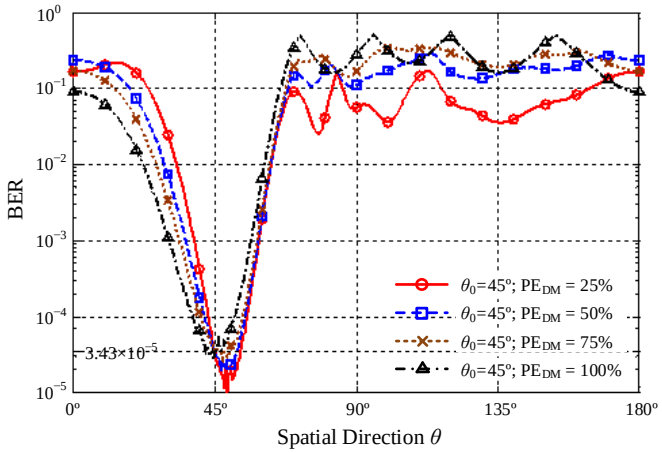

Fig. 6. BER spatial distributions detected by advanced QPSK receivers in the static DM system, designed based on the conventional array and the orthogonal vectors in Table I, with different PE_{DM}s for 45º secure communication.

The above performance limitation associated with advanced

QPSK receiver detection applied to a static DM system can be resolved through by the adoption of dynamic DM transmitter arrays. To show this the BER spatial distributions for dynamic DM systems with different PE_{DM}s for 45º then 90º communications directions are illustrated in Fig. 7. In these cases due to dynamic reallocation of vector sets at each symbol the injected orthogonal vectors can be set to have zero-mean. Therefore the 4 symbol references as recovered from training sequences by advanced QPSK receivers approximately form a standard QPSK constellation pattern. Consequently both basic and advanced receiver types behave equivalently. Compared with static DM, where performance relies largely on the choice of static orthogonal vector sets, dynamic DM provides more consistent performance and is insensitive to receiver functionality. Furthermore BER sidelobes are better suppressed in dynamic DM systems.

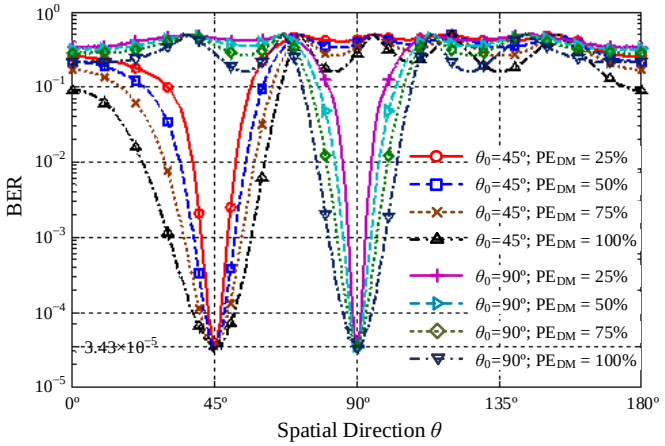

Fig. 7. BER spatial distributions in dynamic DM systems, designed based on conventional array, with different PE_{DM}s for 45º and 90º secure communications.

Similar to traditional non-DM beam steering arrays, the information beam segment for 10^{-3} BER in a dynamic DM array widens when the communications direction is further away from boresight (90º), see Fig. 8.

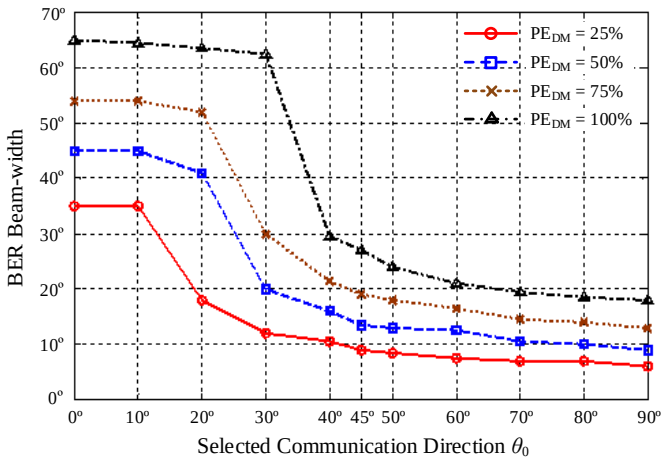

Fig. 8. BER beamwidth for 10^{-3} BER versus selected communication direction θ_0 for different PE_{DM} values.

In a non-DM system, when the channel noise is quite small compared with signal power, there is a chance for eavesdroppers located along sidelobe directions to recover the information data. This high SNR condition can be created by moving eavesdropper receivers closer to the transmitter. In the extreme case, when channel is noise free, equivalent to infinite SNR, the signal can be received and decoded with no error along any spatial directions except in power null directions. However this general broadcast nature can be eliminated by adopting dynamic DM transmitters. To show the superiority that dynamic DM systems possess under high SNR scenarios the BER spatial distributions in dynamic DM systems over a noiseless channel with different PE_{DM}s for 90º communications are depicted in Fig. 9. It can be seen that the BER sidelobes can be effectively suppressed in dynamic DM systems even though wireless channel is noise free. This is because unlike the additive channel noise, the injected orthogonal vectors act as multiplicative interference. If there is no demanding requirement on main BER beam-widths then the power efficiency of the system can be maintained at a high level.

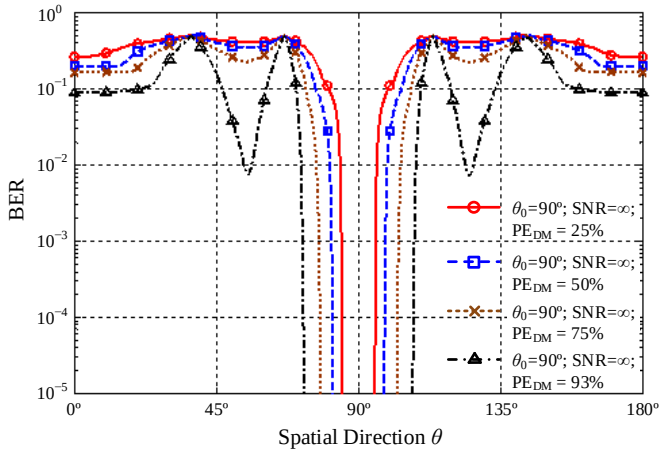

Fig. 9. BER spatial distributions in dynamic DM systems, designed based on conventional arrays, over noiseless channel with different PE_{DM}s for 90º secure communication.

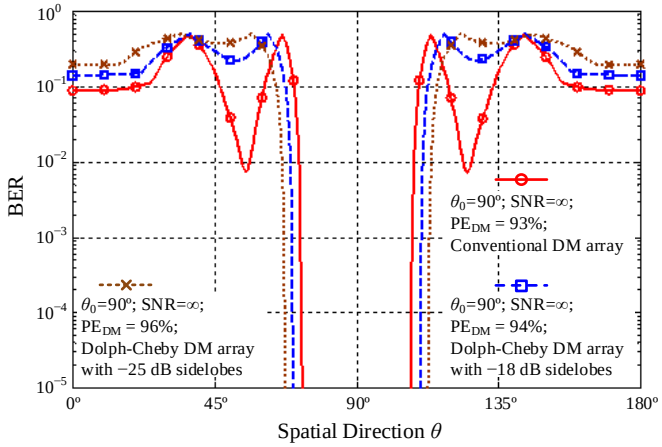

Fig. 10. BER spatial distributions in dynamic DM systems with the same total radiation power, designed based on conventional array and Dolph-Chebyschev arrays, over noiseless channel for 90º communication direction.

If we want to further suppress BER sidelobes while maintaining the same total radiated power a secrecy performance tradeoff between main BER beam-widths and sidelobe levels can be achieved by choosing appropriate non-DM beam steering arrays prior to orthogonal vector injections, e.g., Binomial arrays for lowest sidelobes, Dolph-Chebyschev arrays for controllable and equal sidelobes [23], etc., [24]. In Fig. 10 BER distributions for dynamic DM systems designed based on the conventional array, Dolph-Chebyschev arrays with −18 dB and −25 dB sidelobes for 90º communication are illustrated. For fair comparison, the PE_{DM}s are set to be 93% for the conventional DM array, 94% and 96% for the Dolph-Chebyschev DM arrays with −18 dB and −25 dB sidelobes. These choices for PE_{DM}s lead to an identical total power radiated by each dynamic DM array type. It can be observed from Fig. 10 that rather than increasing the power of the injected orthogonal vectors we have an alternative means to suppress BER sidelobes in extremely high SNR scenarios.

IX. Conclusion

A vector approach allowing analysis and synthesis of DM transmitter arrays was proposed. Using the orthogonal vector concept DM systems can be classified into two categories, static and dynamic. The synthesis methods for both DM system types were presented and verified by BER simulations. Dynamic DM systems where shown to outperform static types and readily lend themselves to digital DM architecture implementation. Experimental verification of the approach suggested here using digital DM architectures will be the subject of later work. The vector synthesis approach introduced in this paper could unlock better DM system solutions ultimately leading to their practical use in applications where enhanced security through physical layer augmentation would add operational benefit.

Acknowledgment

Yuan Ding thanks Mrs. Yi He for useful discussions. The authors also would like to thank the anonymous reviewers for their valuable comments and suggestions.

References

[1] A. Babakhani, D.B. Rutledge and A. Hajimiri, "Transmitter architectures based on near-field direct antenna modulation," *Solid-State Circuits, IEEE Journal of*, vol. 43, pp. 2674-2692, 2008.

[2] A. Babakhani, D. Rutledge and A. Hajimiri, "Near-field direct antenna modulation," *Microwave Magazine, IEEE*, vol. 10, pp. 36-46, 2009.

[3] A. H. Chang, A. Babakhani and A. Hajimiri, "Near-field direct antenna modulation (NFDAM) transmitter at 2.4GHz," in *Antennas and Propagation Society International Symposium*, 2009. APSURSI '09. IEEE, pp. 1-4, 2009.

[4] M. P. Daly and J. T. Bernhard, "Directional modulation technique for phased arrays," *Antennas and Propagation, IEEE Transactions on*, vol. 57, pp. 2633-2640, 2009.

[5] M. P. Daly and J. T. Bernhard, "Beamsteering in pattern reconfigurable arrays using directional modulation," *Antennas and Propagation, IEEE Transactions on*, vol. 58, pp. 2259-2265, 2010.

[6] M. P. Daly, E. L. Daly and J. T. Bernhard, "Demonstration of directional modulation using a phased array," *Antennas and Propagation, IEEE Transactions on*, vol. 58, pp. 1545-1550, 2010.

[7] HongZhe Shi and T. Alan, "Direction dependent antenna modulation using a two element array," in *Antennas and Propagation (EUCAP), Proceedings of the 5th European Conference on*, pp. 812-815, 2011.

[8] Hong Zhe Shi and A. Tennant, "An experimental two element array configured for directional antenna modulation," in *Antennas and Propagation (EUCAP), 2012 6th European Conference on*, pp. 1624-1626, 2012.

[9] C. M. Elam and D. A. Leavy, "Secure communication using array transmitter," *U. S. Patent* 6,275,679, August 14, 2001.

[10] N. Valliappan, 2012: Antenna Subset Modulation for Secure Millimeter-Wave Wireless Communication. *M.S. thesis in Engineering*, The University of Texas at Austin.

[11] T. Hong, M. Z. Song and Y. Liu, "RF directional modulation technique using a switched antenna array for physical layer secure communication applications," *Progress in Electromagnetics Research*, vol. 120, pp. 195-213, 2011.

[12] E. J. Baghdady, "Directional signal modulation by means of switched spaced antennas," *Communications, IEEE Transactions on*, vol. 38, pp. 399-403, 1990.

[13] A. Tennant, "Experimental two-element time-modulated direction finding array," *Antennas and Propagation, IEEE Transactions on*, vol. 58, pp. 986-988, 2010.

[14] Y. S. Poberezhskiy and G. Y. Poberezhskiy, "Efficient utilization of virtual antenna motion," in *Aerospace Conference, 2011 IEEE*, pp. 1-17, 2011.

[15] Tao Hong, Mao-Zhong Song and Yu Liu, "Dual-beam directional modulation technique for physical-layer secure communication," *Antennas and Wireless Propagation Letters, IEEE*, vol. 10, pp. 1417-1420, 2011.

[16] O.N. Alrabadi and G.F. Pedersen, "Directional space-time modulation: A novel approach for secured wireless communication," in *Communications (ICC), 2012 IEEE International Conference on*, pp. 3554-3558, 2012.

[17] C. Balanis, Antenna Theory: Analysis and Design. *John Wiley & Sons, Inc.*, third edition, pp. 290-296, 2005.

[18] R. Negi and S. Goel, "Secret communication using artificial noise," in *Vehicular Technology Conference, 2005. VTC-2005-Fall. 2005 IEEE 62nd*, pp. 1906-1910, 2005.

[19] X. Li, J. Hwu and E. P. Ratazzi, "Using antenna array redundancy and channel diversity for secure wireless transmissions," *Journal of Communications*, Vol. 2, No. 3, Page(s): 24-32, May 2007.

[20] S. Goel and R. Negi, "Guaranteeing secrecy using artificial noise," *Wireless Communications, IEEE Transactions on*, vol. 7, pp. 2180-2189, 2008.

[21] Xiangyun Zhou and M. R. McKay, "Secure transmission with artificial noise over fading channels: achievable rate and optimal power allocation," *Vehicular Technology, IEEE Transactions on*, vol. 59, pp. 3831-3842, 2010.

[22] R.A. Shafik, S. Rahman and AHM Razibul Islam, "On the extended relationships among EVM, BER and SNR as performance metrics," in *Electrical and Computer Engineering, 2006. ICECE '06. International Conference on*, pp. 408-411, 2006.

[23] C. Balanis, Antenna Theory: Analysis and Design. *John Wiley & Sons, Inc.*, third edition, pp. 328-345, 2005.

[24] R. Vescovo, "Consistency of constraints on nulls and on dynamic range ratio in pattern synthesis for antenna arrays," *Antennas and Propagation, IEEE Transactions on*, vol. 55, pp. 2662-2670, 2007.

Yuan Ding received his Bachelor's degree from Beihang University (BUAA), Beijing, China, in 2004 and received his Master's degree from Tsinghua University, Beijing, China, in 2007, both in Electronic Engineering.

He was a RF engineer in Motorola R&D center (Beijing, China) from 2007 to 2009, before joining Freescale semiconductor Inc. (Beijing, China) as a RF field application engineer, responsible for high power base-station amplifier design, from 2009 to 2011. He is currently working toward his Ph.D. degree at the ECIT institute, Queen's University of Belfast, Belfast, United Kingdom. His research interests are in antenna array and physical layer security.

Vincent F. Fusco (S'82–M'82–SM'96–F'04) received the Bachelor's degree (1st class honors) in electrical and electronic engineering, the Ph.D. degree in microwave electronics, and the D.Sc. degree, for his work on advanced front end architectures with enhanced functionality, from The Queens University of Belfast (QUB), Belfast, Northern Ireland, in 1979, 1982, and 2000, respectively.

He holds a personal chair in High Frequency Electronic Engineering at Queens University of Belfast (QUB). His research interests include active antenna and front-end MMIC techniques. He is head of the High Frequency Laboratories at QUB where he is also director of the International Centre for System on Chip for Advanced Microwireless. Professor Fusco has published over 350 scientific papers in major journals and in referred international conferences. He has authored two text books, holds patents related to self-tracking antennas and has contributed invited papers and book chapters.

Prof. Fusco serves on the technical programme committee for various international conferences including the European Microwave Conference. He is a Fellow of both the Institution of Engineering and Technology and the Institute of Electrical and Electronic Engineers. In addition he is a Fellow of the Royal Academy of Engineers and a member of the Royal Irish Academy. In 2012 he was awarded the IET Senior Achievement Award the Mountbatten Medal.